SEMI-EMPIRICAL MODEL FOR STEADY STATE SIMULATION OF DOMESTIC REFRIGERATION SYSTEMS

Cezar O. R. Negrão, negrao@utfpr.edu.br
Raul H. Erthal, rherthal@utfpr.edu.br
Cassio A. Yared, cassioyared@msn.com
Diogo da Vinha Andrade, diogoandrade@hotmail.com
Federal University of Technology – Paraná

Luciana Wasnievski da Silva, Luciana_W_Silva@embraco.com.br
EMBRACO

Abstract. The present work proposes a semi-empirical model to simulate the steady-state behavior of a refrigeration system. The current mathematical model is based on the conservation equations of mass and energy. Parameters, such as, heat transfer coefficients are calibrated with experimental values. As the set of algebraic equations are non-linear, they are solved iteratevely. Some experimental tests were carried out to calibrate the model and also to validate the technique. The results were compared with the experimental data and the temperature differences are within +/-3oC and the compressor power difference lie under 7%.

Palavras-chave*: refrigeration, mathematical model, numerical simulations.*

1. INTRODUCTION

According to Eletrobrás (2004), the residential sector is responsible for 25% of whole energy consumed in Brazil and the domestic refrigeration takes a great part of it. Although the unitary consumption is low - a typical refrigerator consumes about 30kWh/month - 11% of the electricity produced is employed in domestic refrigeration. Therefore, there is a great potential for energy consumption reduction as system efficiency is below 20%.

Experimental tests are the usual practice to evaluate the performance of domestic refrigeration systems, which are conducted within a temperature and humidity controlled chamber. These tests are expensive and quite time consuming. For example, a simple pull-down test is carried out in 24 hours, not considering the system preparation time. The design of refrigeration systems is usually based on previous experience. A new system is built based on resize of components and system optimization. Several tests are then carried out to check its performance, and modifications are conducted according to these tests. Such tial and error approach can take a long time.

The mathematical model of the refrigeration system is an alternative to those tests. With the advent of digital computer, the solution of the system governing equations became feasible. Virtual changes on the system can be conducted but not necessarily they are physically performed (Klein, 1998, Hermes, 2006, Ding 2007). Besides the reduction of the number of experimental tests, the computer simulation is considerably cheaper and faster. The simulation reproduces the system performance not only on the design condition but also on the whole system operation range.

This work presents a mathematical model to simulate the performance of domestic refrigeration systems. The model is base on the governing equations of mass and energy. Conductance and overall heat transfer coefficient values are fitted to measured data.

2. MATHEMATICAL MODEL

The refrigeration system is a domestic vertical freezer which is composed of a hermetic reciprocating compressor, a wire-and-tube condenser, a roll-bond evaporator and a capillary tube, as illustrated in Figure 1. The condenser outlet tube is introduced into the cabinet wall in order to avoid water vapor condensation on the external surfaces of the cabinet. This length of tube in contact with the cabinet external walls forms a hot-wall type condenser. The capillary tube is inserted into the suction line forming a concentric counter-flow heat exchanger.. The system operates at steady state with R134a. Any pressure drop through condenser and evaporator are disregarded. The discharge line temperature is assumed to be equal to the compressor shell temperature, as their values are very close in hermetic compressors.

2.1. Modelling of the System Components

Condenser

Three regions are considered in the condenser: superheating, saturation and sub-cooling. Therefore, the heat rejected by the condenser is the sum of the heat released in each region,

$$\dot{Q}_c = \dot{Q}_{sp,c} + \dot{Q}_{st,c} + \dot{Q}_{sb,c}\ , \tag{1}$$

where $\dot{Q}$ is the heat transfer rate. The subscripts *c*, *sp*, *st* and *sb* stand forcondenser, superheating, saturation and sub-cooling regions, respectively.

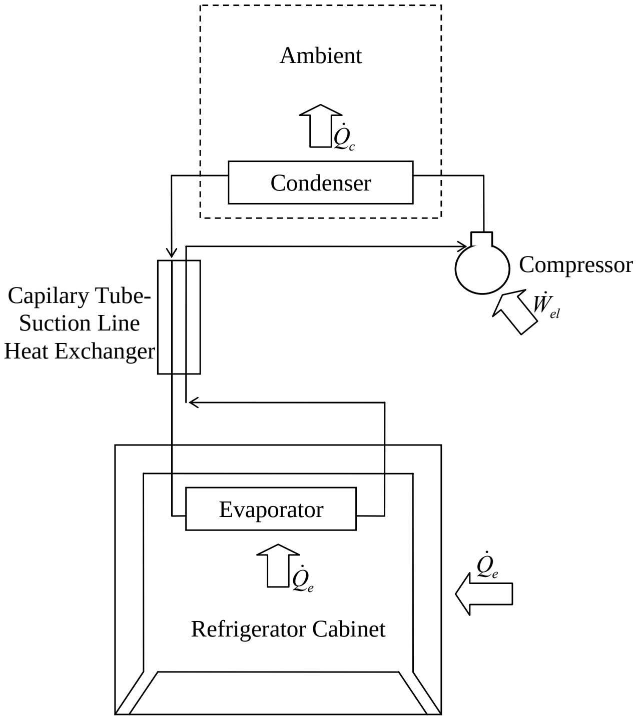

Figure 1. Illustration of the Refrigeration System.

The heat transfer rates in the single-phase regions are modeled according to the definition of effectiveness (Incropera & DeWitt, 2002)

$$\dot{Q}_{sp,c} = \dot{m}\ cp_{sp,c}\left(T_{sh} - T_{\infty}\right)\left(1 - e^{-\frac{U_{sp,c}A_{sp,c}}{\dot{m}\ cp_{sp,c}}}\right) \tag{2}$$

$$\dot{Q}_{sb,c} = \dot{m}\ cp_{sb,c}\left(T_c - T_{\infty}\right)\left(1 - e^{-\frac{U_{sb,c}A_{sb,c}}{\dot{m}\ cp_{sb,c}}}\right) \tag{3}$$

where $\dot{m}$ is the system mass flow rate, T is the temperature, U is overall heat transfer coefficient, A is the heat transfer area and cp is the specific heat. The subscripts *sh* and ∞ refer to discharge line (or compressor shell) and external ambient, respectively. The term inside brackets is the effectiveness. The heat transfer in the condensation region is computed as

$$\dot{Q}_{st,c} = U_{st,c}A_{st,c}(T_c - T_{\infty})\ , \tag{4}$$

where T_c is the condensation temperature. The condenser overall heat transferarea A_c, is given by

$$A_c = A_{sp,c} + A_{st,c} + A_{sb,c}\quad . \tag{5}$$

These heat transfer areas can either be internal or external ones, as they depend on the definition of the overall heat transfer coefficients.

The heat transfer rates can still be calculated according to the energy balances in each region of the condenser, as follows:

$$\dot{Q}_{sp,c} = \dot{m}(h_{sh} - h_{v,c}) \ , \tag{6}$$

$$\dot{Q}_{st,c} = \dot{m}(h_{v,c} - h_{l,c}) \ , \tag{7}$$

$$\dot{Q}_{sb,c} = \dot{m}(h_{o,c} - h_{l,c}) \ , \tag{8}$$

where h is the enthalpy. The subscripts v and l represent saturated vapor and saturated liquid, respectively. The index o is the outlet.

Evaporator

The evaporator is considered to be composed of two regions: saturated and superheated. Thus the heat absorbed by the evaporator is

$$\dot{Q}_e = \dot{Q}_{st,e} + \dot{Q}_{sp,e} \tag{9}$$

where e means evaporator.

The heat transfer rate in the superheating region is computed according to the definition of effectiveness (Incropera & DeWitt, 2002),

$$\dot{Q}_{sp,e} = \dot{m}\ cp_{sp,e} \left(T_e - T_g \right) \left(1 - e^{-\frac{U_{sp,e} A_{sp,e}}{\dot{m}\ cp_{sp,e}}} \right) \tag{10}$$

where the T_g is the average air temperature in the freezer cabinet.

The heat transfer in the evaporation region is given by

$$\dot{Q}_{st,e} = U_{st,e} A_{st,e} (T_e - T_g) \ , \tag{11}$$

where

Asp,e = Ae –Ast,e , (12)

T_e is the evaporation temperature, and Ae isthe evaporator overall heat transfer area.

The heat transfer areas $A_{st,e}$ and $A_{sp,e}$ can either be internal or external ones, as they depend on the definition of the overall heat transfer coefficients.

The heat transfer rate can still be calculated based on energy balances applied to each heat transfer region, as follows:

$$\dot{Q}_{sp,e} = \dot{m}(h_{o,e} - h_{v,e}) \tag{12}$$

$$\dot{Q}_{st,e} = \dot{m}(h_{v,e} - h_{i,e}) \tag{13}$$

where the indices i and o stand for inlet and outlet, respectively.

Capillary Tube

Although the mass flow rate through the capillary tube is enhanced by the heat transfer to the suction line, its value is computed considering the expansion as adiabatic. The conservation equations of mass, momentum and energy are employed to calculate the mass flow rate. The current model is based on the Boabaid Neto´s (1994) work and a general form for the calculations of the mass flow rate is written as a function of condensation and evaporation pressures and the condenser outlet enthalpy:

$$\dot{m} = \dot{m}(p_c , p_e , h_{o,c} , \dot{Q}_{tc}) \tag{14}$$

Capillary Tube-Suction Line Heat Exchanger

The energy balance on the capillary tube and on suction line provide the following expressions for the heat exchanged rate:

$$\dot{Q}_{tc} = \dot{m}(h_{o,c} - h_{i,e}) \tag{15}$$

$$\dot{Q}_{tc} = \dot{m}(h_{o,tc} - h_{o,e}) \tag{16}$$

where t_c is the capillary tube-suction line (CT-SL) heat exchanger. The flow temperature at the capillary tube varies not only because of the heat exchange but also because of the flow expansion (Yang & Bansal, 2005). For heat exchange calculation purpouse, the expansion effect on the temperature drop is neglected, and therefore, the concept of heat exchanger effectiveness is once again used as follows:

$$\dot{Q}_{tc} = \dot{m}\, cp_{sp,e} (T_{o,c} - T_{o,e})\varepsilon_{tc} \, . \tag{17}$$

$T_{o,c}$ and $T_{o,e}$ are the condenser and evaporator outlet temperatures, respectively. The effectiveness of a counter flow heat exchanger can be computed by (Incropera & DeWitt, 2002),

$$\varepsilon_{tc} = \frac{1 - e^{-NTU(1+C_r)}}{1 - C_r e^{-NTU(1-C_r)}} \quad , \tag{18}$$

where $NTU = \frac{U_{tc} A_{tc}}{\dot{m} cp_{sp,e}}$ e $C_r = \frac{cp_{sb,c}}{cp_{sp,e}}$. U_{tc} and A_{tc} are the overall heat transfer coefficient and the heat transfer area of the heat exchanger, respectively. It was assumed that both the capillary tube and the suction line do not exchange heat with the neighborhood.

Freezer Cabinet

The heat transfer rate through the freezer cabinet is computed by the Newton´s law of cooling:

$$\dot{Q}_e = U_g A_g (T_g - T_\infty) \tag{19}$$

At steady state, such heat transfer rate is equal to the system refrigerating capacity.

Compressor

An overall energy balance applied to the compressor shell results in

$$\dot{m}(h_d - h_{o,tc}) + \dot{W}_{el} = \dot{Q}_{sh} \tag{20}$$

where $h_{o,tc}$ is enthalpy at the compressor suction line (or the CT-SL heat exchanger outlet temperature), $\dot{W}_{el}$ is the compressor power, and $\dot{Q}_{sh}$ is the heat reject to the neighborhood, which is determined by

$$\dot{Q}_{sh} = U_{sh} A_{sh} (T_{sh} - T_\infty) \tag{21}$$

T_{sh} is the average shell temperature.

A semi-empirical model is proposed to evaluate the mass flow rate and compressor power. The compressor mass flow rate $\dot{m}$ is computed according to the following relation:

$$\dot{m} = B \cdot \frac{PD}{v_s} \left\{ 1 - C \left[\left(\frac{p_c}{p_e} \right)^{1/k} - 1 \right] \right\}, \tag{22}$$

where PD is the piston displacement, v_s is the specific volume at the compressor inlet, C is the clearance fraction, p_c is the discharge/condensation pressure, p_e is the suction/evaporation pressure and k is the isentropic coefficient. To evaluate the specific volume, it was assumed that the compressor inlet temperature is approximately equal to the compressor shell temperature. The parameter B that represents the ideal-to-actual volumetric efficiency ratio, is fitted to calorimeter data. A comparison of experimental and theoretical values of mass flow rate shows that B values are linearly dependent on the pressure ratio. This relation is given by

$$B = a_1 + b_1\left(\frac{P_c}{P_e}\right) \tag{23}$$

where and a_1 and b_1 are constants, and their values are shown in Table 1, for two compressor models (A and B). Note that a_1+b_1 is close to 1, and therefore, as p_c/p_e approaches 1, the actual volumetric efficiency approaches its ideal counterpart. On the other hand, the greater the pressure ratio, the lower the B value. In other words, the actual volumetric efficiency reduces in comparison to the ideal one, as leakage increase with the pressure ratio. Table 1 also shows the correlation coefficient (R^2) and the larger difference between the measured and calculated mass flow rates.

The comparison of the compressor power and the isentropic compression power showed they are linearly related, as follows:

$$\dot{W}_{el} = a_2 + \frac{\dot{m}w_i}{b_2} \;, \tag{24}$$

where a_2 and b_2 are constant values, also shown in Table 1, together with the correlation coefficient and the larger difference between the measured and calculated compressor power for two compressor models. The isentropic compression work w_i is (Gosney, 1982):

$$w_i = p_e v_{sh}\frac{k}{k-1}\left[\left(\frac{p_c}{p_e}\right)^{\frac{k-1}{k}} - 1\right] \tag{25}$$

According to equation (25), $W_{el} \sim a_2$, as $\dot{m}$ or w_i approaches zero. Therefore, a_2 represents a no-load power or all the mechanical and electric losses. b_2, on the other hand, is the thermodynamic efficiency.

Nine calorimeter tests were conducted at EMBRACO laboratories in order to fit the constants a_1, b_1, a_2 and b_2. Mass flow rate, compressor power and compressor shell temperature were measured for three different condensation (45^{o}C, 55^{o}C and 60^{o}C) and three different evaporation (-35^{o}C, -25^{o}C and -15^{o}C) temperatures.

Table 1. Fitted constants of equations (23) and (24) for two compressor models.

Compressor	Mass flow rate				Compressor Power			
	a_1 (-)	b_1 (-)	R^2	Larger Difference [%]	a_2 (W)	b_2 (-)	R^2	Larger Difference [%]
A	1.0282	-0.01781	0.985	-2.5	31.59	0.7860	0.997	2.8
B	1.0579	-0.01733	0.971	4.6	25.09	0.9398	0.999	1.5

2.2 Thermodynamic Properties

Thermodynamic correlations are used to complete the set of equations defined above. A table with all required thermodynamic properties is built using REFPROP (NIST, 2007). This table is stored in the computer hard disk as a file and it is read when the simulation takes place. During the simulation, second order interpolations are carried out as necessary.

2.3. Model Calibration

In the current model, the conductance (*UA* values) from equations (2), (3), (4), (10), (11), (18), (19) and (21) are calibrated using experimental data..

The freezer cabinet conductance in equation (19) is computed by a specific test. The air inside the freezer cabinet is heated with an electric heater. The heater electric power and the inside and outside air temperatures are measured. Equation (19) is then solved for $(UA)_g$. The other conductance values are obtained from a stabilized condition of a pull-down test performed in a 25^{o}C, 32^{o}C and 43^{o}C temperature controlled chamberBesides temperature, pressure and compressor power, the mass flow rate was also measured by a Coriolis-type flowmeter. These experiments were conducted at POLO Laboratories[1].

As the magnitude of the condenser and evaporator two-phase and single-phase areas may be modified from test to test, the conductance may also change. Assuming the overall heat transfer coefficients are little affected by the operating conditions, these coefficients are computed rather than the conductance. An exception is the condenser sub-cooling region, as the hot-wall condenser area is unknown. The sub-cooling is considered to take place only in that part of the condenser.

Table 2 presents the calibrated overall heat transfer coefficients and conductance values for equations (2), (3), (4), (10), (11), (18), (19) and (21). One can see the conductance is considerably affected by the ambient temperature. The effect of the conductance on the simulation results is discussed in section 3.0.

Table 2. Calibrated values of overall heat transfer coefficients and conductance.

Overall heat transfer coefficients (W/m^2K)	25^oC	32^oC	43^oC	Conductance (W/K)	25^oC	32^oC	43^oC
$U_{sp,c}$	4.3	13,3	28.5	$(UA)_{tc}$	0.61	0.70	0.57
$U_{st,c}$	45.3	46.3	51.1	$(UA)_{sh}$	1.69	1.73	1.86
$(UA)_{sb,c}$	0.17	0.15	0.25	$(UA)_g$	1.165	1.207	-
$U_{sp,e}$	11.2	14.0	20.2				
$U_{st,e}$	5.5	5.7	6.3				

2.3. Solution Method

The set of equations (1) to (25), together with thermodynamic correlations, must be solved in order to obtain the values of temperature, pressure, mass flow rate and compressor power. An iterative procedure is employed to solve such equations. The condensation and evaporation temperatures, as well as the compressor inlet temperature are initially fixed. The compressor mass flow rate, power and shell temperature can thus be computed. The mass flow rate is used to evaluate the heat transfer in the condenser superheating, saturation and sub-cooling regions and also the condenser outlet condition. With the condensation and evaporation pressures, and the condenser outlet condition, the mass flow rate through the capillary tube is calculated. As the condensation and evaporation temperatures were guessed, the compressor and capillary tube mass flow rates are not the equal. The condensation temperature is thus changed according to the difference of the compressor and capillary tube mass flow rates. If this difference is positive, the condensation temperature is increased. The compressor mass flow rate and compressor shell temperature is again computed, and this iterative procedure continues until the difference between the compressor and the capillary tube mass flow rates is under the convergence criterion. Next, the CT-SL heat exchanger equations are solved and the evaporator inlet condition is determined. The evaporator heat transfer rate is employed to compute the cabinet average temperature. This temperature is thus used to calculate the heat transfer rate through the cabinet walls, which is compared to the evaporator heat transfer rate. If they are different, the evaporation temperature is corrected, and a new iteration starts.

In the solution, the evaporator outlet condition is fixed (the superheating or the refrigerant quality). This is an alternative to the mass distribution evaluation within the refrigeration system. The mass inventory is one of the main shortcomings in refrigeration systems modeling because of the two-phase flow in evaporators and condensers. Void fraction models found in the literature are usually not appropriate to predict the correct mass distribution in such systems.

3. RESULTS

In order validate the model, simulations were conducted for three different ambient temperatures: 25^oC, 32^oC and 43^oC and the results were compared with measured values. Two compressors were tested: compressors A and B of Table 1. The conductance and overall heat transfer coefficients employed in the simulations are those computed for the ambient temperature of 32^oC (see Table 2). Evaporation is considered to take place along almost the whole evaporator, and therefore, a 6.0^oC superheating at the evaporator outlet is assumed for all simulations.

Table 3 shows measured and computed values for the system working with compressor A. A good agreement of results is seen at 32^oC. Most of the temperature differences are under +/-2.0^oC and the differences of other quantities lay under -5.0% to +7.0%. Two are the cases where temperature differences are larger than 2.0^oC: the compressor shell and evaporator outlet temperatures. The first is related to the assumption that compressor shell temperature is equal to the

[1] POLO Laboratories – Refrigeration and Thermophysics Research Laboratories, Department of Mechanical Engineering, Federal University of Santa Catarina.

discharge temperature, while the latter is related to the fact that superheating at the evaporator outlet is fixed for all simulations. That means the model calibration is quite adequate.

Two measured refrigerating capacity values are presented in Table 3: the first is the product of the mass flow rate and evaporator enthalpy difference, and the second is the product of the cabinet conductance and the inside and outside cabinet temperature difference. These differences are -3.6% and 2.2%, respectively.For ambient of 25°C and 43°C, the differences between measured and computed temperatures are within +/-2.0°C and +/-3,0°C, respectively. Excepting for the refrigerating capacity at 43°C, the other differences are below 7%. The -9.4% refrigerating capacity discrepancy can be due to the calculation of the refrigerating capacity by the enthalpy differences. As the evaporator is a roll-bond type and the CT-SL heat exchanger ends at the evaporator plate, the evaporator outlet condition is not precisely defined. However, the results from simulation, in general, have presented a good agreement with the ones from experiment, indicating that the conductance and the overall heat transfer coefficient variations (see values in Table 2) do not significantly affect the results.

Data for compressor B are shown in Table 4. The same values of conductance and overall heat transfer coefficients evaluated at 32ºC, and shown in Table 2, were employed. Differences in temperature were found between -2.0°C and +3.0°C, while for mass flow rate the differencesare in the order of -6% for 25°C and 32°C, and 9.0% for 43°C. On the other hand, for compressor power these values were below 4% for all ambient temperatures. The difference between the computed refrigerating capacity and the product of mass flow rate and enthalpy difference has increased, compared to results from Table 3. The refrigerating capacities obtained from the product of UA and the temperature difference are in good agreement with simulation results.

Table 3 – Comparison of simulation and measuring results for compressor A.

	Meas.	Comp.	Diff.	Meas.	Comp.	Diff.	Meas.	Comp.	Diff.
Variable	25°C			32°C			43°C		
Compressor shell temperature (°C)	67.5	69.1	-1.6ºC	76.2	78.2	-2.0ºC	90,6	92,9	2,3ºC
Condenser outlet temperature (°C)	32,8	33,1	-0.3ºC	40.9	41.2	-0.3ºC	51,8	53,8	2,0ºC
Evaporator outlet temperature (°C)	-33.9	-35.6	1.7ºC	-30.4	-32.6	2.2ºC	-25.0	-27.7	-2.7ºC
Cabinet average temperature (°C)	-32,6	-34.0	1.4ºC	-29.2	-30.6	1.4ºC	-24.1	-25.0	-0.9ºC
Evaporation temperature (°C)	-40.5	-41.6	1.2ºC	-37.6	-38.6	1.0ºC	-32.7	-33.7	-1.0ºC
Condensation temperature (°C)	35.2	34.5	0.7ºC	43.0	42.5	0.5ºC	54.7	53.7	-1.0ºC
Evaporation pressure (bar)	0.50	0.47	-6.0%	0.58	0.55	-5.2%	0.74	0.71	-4.2%
Condensation pressure (bar)	8.93	8.87	-0.7%	11.0	10.9	-1.3%	14.8	14.6	-1.2%
Mass flow rate (kg/h)	1.50	1.49	-0.7%	1.71	1.65	-3.5%	2.08	1.96	-6.1%
Compressor power (W)	80.4	85.9	6.8%	87.4	93.8	7.3%	103.2	108.7	5.1%
Refrigerating capacity (W)	71.3/69.5	71.3	0.0/2.6%	78.2/73.9	75.5	-3.5/2.2%	89.8/81.0	82.1	-9.4/1.4%
Condenser heat transfer rate (W)	84.0	85.2	3.3%	93.4	92.3	-1.1%	110.6	104.9	-5.5%
CT-SL Heat transfer rate (W)	17.5	17.0	-2.6%	19.7	19.8	0.5%	28.8	24.8	-13.0%

4. CONCLUSIONS

This work presented a semi-empirical model for the steady state simulation of refrigeration systems. The model was based on conductance and overall heat transfer coefficients obtained from measured data. A theoretical compressor model was fitted to compressor calorimeter data. The system set of algebraic equations were solved iteratively. The solution methodology was quite robust as divergence has not been found for all tested cases. It was shown that the conductance and overall heat transfer coefficients vary quite significantly with the ambient temperature. These calibrated coefficients were employed to simulate the refrigeration system in different ambient temperatures, and the results presented good agreement with measured values, for both compressors tested. The differences in temperature were found between -2.0°C and +3.0°C and the differences of other quantities were between -5.0% and +7.0%. All the simulations were carried out with the same set of conductance and overall heat transfer coefficients; the ones obtained at 32°C, and it was observed that the changes of conductance and overall coefficients with ambient temperature do not affect significantly the simulation results. One can see that the performance of each system component was well characterized by the conductance or overall heat transfer coefficients, which can be evaluated by a single test. Thus, is a simple method was presented to compute the whole system performance in different ambient temperatures or with a different compressor.

Table 4- Comparison of simulation and measuring results for compressor B.

	Meas.	Comp.	Diff.	Meas.	Comp.	Diff.	Meas.	Comp.	Diff.
Variable	25°C			32°C			43°C		
Compressor shell temperature (°C)	58.9	60.9	-2,0ºC	68.2	69.4	-1.2ºC	85.8	84.2	1.6ºC
Condenser outlet temperature (°C)	32.4	33.1	-0.7ºC	40.2	41.1	-0.9ºC	50.8	53.7	-2.9ºC
Evaporator outlet temperature (°C)	-36.0	-36.3	0.3ºC	-32.2	-32.9	0.7ºC	-26.2	-28.4	2.2ºC
Cabinet average temperature (°C)	-34.6	-34.6	0.0ºC	-31.1	-30.8	-0.3ºC	-25.6	-25.7	0.1ºC
Evaporation temperature (°C)	-43.3	-42.3	-1.0ºC	-40.8	-38.9	-1.9ºC	-34.4	-34.4	0.0ºC
Condensation temperature (°C)	35.1	35.1	0.0ºC	43.5	42.4	1.1ºC	54.8	54.2	0.6ºC
Evaporation pressure (bar)	0.43	0.45	4.4%	0.51	0.54	5.6%	0.68	0.68	0.0%
Condensation pressure (bar)	8.89	8.88	-0.1%	11.1	10.8	-2.9%	14.8	14.6	-1.3%
Mass flow rate (kg/h)	1.60	1.50	-6.3%	1.77	1.66	-6.2%	2.17	1.98	-8.8%
Compressor power (W)	69.5	68.2	-1.9%	76.9	74.2	-3.5%	91.9	88.2	-4.0%
Refrigerating capacity (W)	76.3/71.9	72.0	-5.7/0.1%	81.7/76.2	75.8	-7.2/-0.5%	94.9/82.8	82.9	-12.7/-0.5%
Condenser heat transfer rate (W)	82.5	82.7	0.3%	94.96	88.5	-6.8%	113.8	100.8	-11.4%
CT-SL Heat transfer rate (W)	22.7	17.3	-23.8%	21.10	19.9	-5.7%	28.2	25.1	-11.0%

5. ACKNOWLEDGEMENTS

The authors acknowledge the financial support of EMBRACO and CNPq (PIBIC – Program).

6. REFERÊNCIAS

Boabaid Neto, C., 1994, "Performance Analysis of Adiabatic Capillary Tubes", MSc Thesis, Department of Mechancail Engineering, Federal University of Santa Catarina, Florianópolis, Brazil. (in Portuguese)

Ding, G., 2007, "Recent developments in simulation techniques for vapour-compression refrigeration systems". International Journal do Refrigeration Vol.30, pp. 1119 – 1133.

Hermes, C.J.L., 2006, "A Methodology for Transient Simulation of Domestic Refrigeration Systems", PhD Thesis, Department of Mechancail Engineering, Federal University of Santa Catarina, Florianópolis, Brazil. (in Portuguese)

Incropera, F.P. and DeWitt, D.P., 2002, Fundamentals of Heat and Mass Transfer, fifth edition, John Wiley & Sons, Inc.

Klein, F.H., 1998, "Development of Computational Code for the Analysis of the Performance of Domestic Refrigertion Systems", MSc Thesis, Department of Mechancail Engineering, Federal University of Santa Catarina, Florianópolis, Brazil. (in Portuguese)

NIST, 2007, "Reference Fluid Thermodynamic and Transport Properties Database (REFPROP)". Version 7.0

Stoecker, W.F. and Jones, J.W., 1982, "Refrigeration and Air Conditioning", MyGraw-Hill, Inc.

Yang, C., Bansal, P. K., 2005, "Numerical investigation of capillary tube-suction line heat exchanger performance", Applied Thermal Engineering, Vol. 25, pp. 2014-2028.

7. RESPONSIBILITY NOTICE

The authors are the only responsible for the printed material included in this paper.